Intramyocellular Ceramides: Subcellular Concentrations and Fractional De Novo Synthesis in Postabsorptive Humans

Jin Ook Chung,[1,2] Christina Koutsari,[1] Agnieszka U. Blachnio-Zabielska,[3] Kazanna C. Hames,[1] and Michael D. Jensen[1]

Diabetes 2017;66:2082–2091 | https://doi.org/10.2337/db17-0082

METABOLISM

We investigated the relationship between insulin resistance markers and subsarcolemmal (SS) and intramyofibrillar (IMF) ceramide concentrations, as well as the contribution of plasma palmitate (6.5-h infusion of [U-^{13}C]palmitate) to intramyocellular ceramides. Seventy-six postabsorptive men and women had muscle biopsies 1.5, 6.5, and 24 h after starting the tracer infusion. Concentrations and enrichment of muscle ceramides were measured by liquid chromatography-tandem mass spectrometry. We found that HOMA of insulin resistance, plasma insulin, and triglyceride concentrations were positively correlated with SS C16:0 and C18:1 ceramide, but not SS C14:0-Cer, C20:0-Cer, C24:0-Cer, and C24:1-Cer concentrations; IMF ceramide concentrations were not correlated with any metabolic parameters. The fractional contribution of plasma palmitate to 16:0 ceramide was greater in SS than IMF (SS, 18.2% vs. IMF, 8.7%; *P* = 0.0006). Plasma insulin concentrations correlated positively with the fractional contribution of plasma palmitate to SS 16:0 ceramide. The fractional contribution of plasma palmitate to intramyocellular SS 16:0 ceramide was positively correlated with SS C16:0 ceramide concentrations (γ = 0.435; *P* = 0.002). We conclude that skeletal muscle SS ceramides, especially C16 to C18 chain lengths and the de novo synthesis of intramyocellular ceramide from plasma palmitate are associated with markers of insulin resistance.

Ceramides are a family of hydrophobic molecules comprising a variable-length fatty acid linked to a sphingosine base. They are well recognized as structural components of cellular membrane (1,2), but are also signaling molecules that are implicated in insulin resistance (1,2). Some investigators find that skeletal muscle ceramide content is elevated in obese, insulin-resistant humans (3,4). However, most studies have focused on the ceramide contents in total skeletal muscle, whereas there is evidence that the subcellular localization of lipid molecules is important (5). Skeletal muscle can be separated into different fractions, including the subsarcolemmal (SS) and intramyofibrillar (IMF) compartments, where distinct lipid and protein compositions in each fraction might contribute to different physiologic processes (6). Because the negative effects on the insulin signaling pathway are mostly restricted to the plasma membrane (7), the subcellular localization of ceramides may be involved in insulin resistance and metabolic abnormalities. In addition, in vitro studies have suggested that the chain length of the fatty acid added to sphinganine results in distinct biologic actions (8); whether there are relationships between different intramyocellular ceramide species and insulin resistance markers in humans has not been fully clarified.

In postabsorptive conditions, circulating free fatty acids (FFA) released from adipose tissue and triglyceride-rich lipoproteins originating from the liver are taken up by skeletal muscle (9). Because the activity of serine palmitoyltransferase, the rate-limiting step of ceramide biosynthesis, depends on palmitoyl-CoA availability, FFA likely contribute to de novo synthesis of intramyocellular ceramides (1,2). However, the contribution of FFA to subcellular ceramide synthesis in postabsorptive human skeletal muscle is

[1]Endocrine Research Unit, Mayo Clinic, Rochester, MN
[2]Department of Internal Medicine, Chonnam National University Medical School, Gwangju, Korea
[3]Department of Hygiene, Epidemiology and Metabolic Disorders, Medical University of Białystok, Białystok, Poland

Corresponding author: Michael D. Jensen, jensen.michael@mayo.edu.

Received 16 January 2017 and accepted 30 April 2017.

This article contains Supplementary Data online at http://diabetes.diabetesjournals.org/lookup/suppl/doi:10.2337/db17-0082/-/DC1

unknown. By using a labeled ([U-^{13}C]palmitate) FFA tracer, it is possible to determine the fate of plasma palmitate within muscle tissue (10). We hypothesized that differences in the de novo synthesis of ceramides in SS and/or IMF of skeletal muscle would be related to markers of insulin resistance in humans.

The aim of this study was to assess whether subcellular locations and species of ceramides in skeletal muscle relate to markers of insulin resistance in postabsorptive humans. In addition, we explored the effects of insulin-resistant conditions on fractional contribution of plasma palmitate to intramyocellular ceramides. Lastly, we investigated the relationship between ceramide concentration and fractional contribution of plasma palmitate to intramyocellular ceramide.

RESEARCH DESIGN AND METHODS

The study was approved by the Mayo Clinic Institutional Review Board. Informed, written consent was obtained from all volunteers.

Participants

We included weight-stable, healthy volunteers (29 men and 47 premenopausal women) who were taking no medications, including oral contraceptives. Participants were recruited to represent a wide range of BMIs (20–36 kg/m^2). Prior to the studies, we documented that each volunteer had a normal complete blood count and chemistry group.

Study Protocol

The experimental design of the current study is provided in Fig. 1. Participants received all of their meals (50% carbohydrate, 35% fat, and 15% protein) from the Mayo Clinic Clinical Research Unit (CRU) metabolic kitchen for 5 days prior to the study to ensure stable energy intake. Volunteers were admitted to the CRU at 1700 h and given a meal at 1800 h. At 0545 h the next day, a forearm vein catheter was inserted and kept patent with a controlled infusion of 0.45% NaCl, and a second catheter was placed in a retrograde fashion in a hand vein for collecting arterialized blood using the heated hand vein technique. After collecting a baseline blood sample for background palmitate enrichment, we started a continuous infusion of [U-^{13}C]palmitate (2–4 nmol/kg fat-free mass [FFM]/min) (Cambridge Isotope Laboratories, Andover, MA) at 0700 h. After 30 min for isotopic equilibration, a series of four blood samples was collected at 10-min intervals and then every 30 min until 1330 h to measure palmitate kinetics. Muscle biopsies were collected at 0830 (first biopsy) and 1330 h (second biopsy) from the vastus lateralis under local anesthesia (2% lidocaine/8.9% sodium bicarbonate [3:1]) using sterile technique. The volunteers remained in bed between biopsies, but were asked to move both legs every 15 min to avoid complete immobility. A third muscle biopsy was collected the next morning at 0800 h, and the participants were then dismissed from the CRU.

The muscle tissue was immediately washed of blood using an ice-cold normal saline solution, dissected of all visible adipose tissue, further rinsed of lipid droplets, and saved immediately in liquid N_2. Samples were stored at −80°C until analysis.

Body Composition Measurements

Total and regional fat masses were assessed with DXA (Lunar Radiation, Madison, WI). Leg fat mass was considered lower-body subcutaneous (LBSQ) fat. Visceral fat mass was estimated using a combination of single-slice computed tomography (L2–L3 interspace) and DXA-measured abdominal fat (11). Total body fat minus visceral and LBSQ fat masses was upper-body subcutaneous fat mass.

Assays

Plasma Analyses

A Beckman Instrument (Fullerton, CA) was used to measure plasma glucose. Plasma palmitate concentration and enrichment were measured using a liquid chromatography-mass spectrometry method (12). Plasma triglyceride concentrations were measured by a microfluorometric method (13).

Muscle Analyses

Muscle lipids were measured after the frozen samples were dissected free of extramyocellular adipocytes while being kept at 0°C on dry ice (14). The muscle was then pulverized

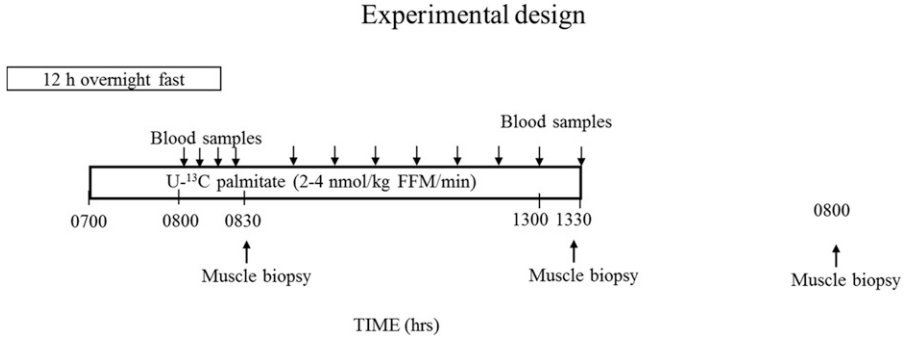

Figure 1—Schematic study design. Time is shown as clock time.

into a fine powder by using a stainless steel mortar and pestle on dry ice (14). We analyzed the SS and IMF fractions. To do this, we homogenized ~100 mg muscle in 1,000 μL homogenization buffer (0.25 mol/L sucrose [S 5–500], 25 mmol/L KCl, 50 mmol/L Tris [T 87,602], and 0.5 mmol/L EDTA [E 4,884]; pH 7.4) at a tissue to buffer ratio of 1:10. After homogenizations, we transferred 800 μL homogenate to a new 1-dram vial.

For the 800-μL homogenate used for SS and IMF fractionation, we centrifuged the sample for 10 min (4°C) at 2,000 rpm. The supernatant was used as the SS fraction and the pellet for the IMF fraction.

The mitochondrial characteristics of these fractions have been reported (15,16), but we found little information regarding the representation of cytosolic and membrane proteins in these two fractions. Therefore, capillary Western analyses were performed using the ProteinSimple Wes System to determine the relative amounts of Na/K ATPase α1 (antibody #23565; Cell Signaling Technology, Danvers, MA), a marker of plasma membranes, and GAPDH (antibody #2118; Cell Signaling Technology), a cytosolic marker, in these two fractions.

We transferred the supernatant containing the SS fraction to a new vial, added 10 μL internal standard mix (17C Sph, 17C S1P, and C17-Cer), vortexed, measured the protein concentration in a 3-μL aliquot, and extracted the compounds of interest with isopropanol/water/ethyl acetate at a ratio of 30:10:60 in the remaining aliquot. For the pellet containing the IMF fraction, we added 800 μL homogenization buffer to resuspend the pellet and then processed the sample as outlined above.

Intramyocellular ceramide concentrations and enrichments were measured by liquid chromatography-tandem mass spectrometry as previously described (10). Our enrichment standard curve is reproducible for total ceramide enrichments at or somewhat <0.01% (10). The concentration standard curve included the following ceramide species: C14:0-Cer, C16:0-Cer, C18:1-Cer, C18:0-Cer, C20:0-Cer, C24:0-Cer, and C24:1-Cer. Subsequent to the analysis of these samples, we learned that there is differential extraction of long-chain ceramides (C20 and longer) and the shorter-chain ceramides, such that using the C17-Cer C18:0 internal standard systematically overestimated long-chain ceramide concentrations. This problem can be overcome by the use of a 17C-Cer C24:0 internal standard, which unfortunately was not available at the time we processed these samples. Thus, the C20:0-Cer, C24:0-Cer, and C24:1-Cer concentrations we found are systematically greater than the concentrations that are present in muscle when assayed with the very-long-chain ceramide internal standard.

Statistical Analysis

Data are represented as the mean ± SD or median (interquartile ranges), unless otherwise noted. Variables with skewed distributions were log-transformed prior to analysis. Differences in the values between IMF and SS fraction were made using Wilcoxon signed-rank test or paired *t* test. Correlations between measurements were determined using Pearson correlation analysis. The M+16 enrichment in 16C ceramide was divided by the plasma palmitate M+16 enrichment to determine the fraction of intramyocellular ceramides that were derived from newly arrived plasma palmitate via the de novo synthesis pathway. Differences in intramyocellular [$^{13}C_{16}$]16:0 ceramide enrichment were made using repeated-measures Friedman test. Differences in fractional contributions of plasma palmitate to intramyocellular ceramide between the first and second biopsy were made using Wilcoxon signed-rank test, and differences between the fractions were determined using Wilcoxon signed-rank test and adjusted for multiple comparisons. For evaluation of statistical significance with three different groups of ceramides according to chain length of ceramide (medium [C14], long [C16–18], and very long [C20–24] chain) in the two fraction groups, a modified Bonferroni method was used to correct for multiple comparisons, with a significant *P* value of <0.0083. For statistical significance, other than associations with ceramide subspecies, an α level of 0.05 was used. Stepwise multiple linear regression analyses were performed to determine the association between metabolic parameters and intramyocellular ceramide species and between metabolic parameters and fractional contribution of plasma palmitate to intramyocellular ceramide. Variance inflation factor was used to detect multicollinearity. A variance inflation factor >10 was excluded from the model. Statistical analysis was performed using SPSS software (SPSS version 20.0; SPSS, Inc., Chicago, IL).

RESULTS

Subject Characteristics

The characteristics of the participants are provided in Table 1. The average age of the participants was 35 years, and the average BMI was 27.7 kg/m^2. The mean fasting plasma insulin concentration was 5 μIU/mL. The average plasma palmitate concentrations and enrichments between 0 and 90 min (prior to the first biopsy) and 210–330 min (prior to the second biopsy) are also provided in Table 1. Supplementary Fig. 1 depicts the mean of all available data at each time point for which the measurement was made. Because palmitate concentrations, enrichments, and therefore flux were relatively stable, the enrichments over the time interval between the two biopsies were used to derive the fractional contribution of plasma palmitate to de novo C16:0 ceramide.

Muscle Protein Characterization

The proportion of muscle protein present in SS and IMF fractions averaged 25 ± 7 and 75 ± 7%, respectively, for these samples. Because we did not have protein remaining from these samples to measure the relative content of Na/K ATPase α1 and GAPDH, we processed new muscle samples using the same technique and subjected the aliquots to capillary Western analysis. Equal amounts of protein were loaded for each of the fractions for each marker, although

Table 1—Subject characteristics

	Total (n = 76)
Age (years)	35 ± 8
BMI (kg/m^2)	27.7 ± 5.2
Glucose (mg/dL)	90 (86–94)
Insulin (μIU/mL)	5 (3–8)
HOMA-IR	1.08 (0.80–1.68)
Total cholesterol (mg/dL)	173 ± 33
HDL cholesterol (mg/dL)	56 ± 14
Triglycerides (mg/dL)	75 (61–103)
Fat (%)	33.3 ± 11.5
FFM (kg)	52.0 ± 11.5
UBSQ fat (kg)	21.9 ± 6.1
LBSQ fat (kg)	10.1 ± 4.9
Visceral fat (kg)	1.7 (1.1–3.3)
Plasma palmitate (0–90 min) (μmol/L)	118 ± 29
Plasma palmitate (150–330 min) (μmol/L)	115 ± 28
Plasma palmitate R_a (60–90min) (μmol/min)	126 ± 44
Plasma palmitate R_a (210–330min) (μmol/min)	131 ± 45

Data are mean ± SD or median (interquartile range). The plasma palmitate concentrations and enrichment values in this table are calculated such that each participant contributed one average value to the overall mean for each interval. That value was the mean of all of the data points collected during that interval. We were not able to collect all of the planned samples from every volunteer. R_a, rate of appearance; UBSQ, upper-body subcutaneous.

Table 2—Intramyocellular ceramide concentrations according to subcellular fraction

Ceramide (pmol/mg protein)	SS fraction	IMF fraction	P value
Total Cer	74.8 (64.5–86.3)	45.4 (36.5–52.0)	<0.0001
C14:0-Cer	0.22 (0.17–0.29)	0.24 (0.20–0.31)	0.096
C16:0-Cer	8.4 (6.3–10.3)	5.0 (4.1–6.1)	<0.0001
C18:1-Cer	5.0 (3.6–6.4)	5.2 (4.2–6.8)	0.394
C18:0-Cer	31.3 ± 9.6	20.5 ± 9.9	<0.0001
C20:0-Cer	0.94 (0.76–1.16)	0.13 (0.08–0.28)	<0.0001
C24:1-Cer	4.9 (3.6–7.3)	1.7 (1.3–2.2)	<0.0001
C24:0-Cer	23.4 (19.9–27.3)	12.2 (10.9–15.1)	<0.0001

Data are mean ± SD or median (interquartile range). Intramyocellular ceramide concentrations are the average from the three biopsies and normalized to milligrams protein. Analyzed by Wilcoxon signed-rank test or paired t test.

the assay for GAPDH required one-tenth the amount of protein as did the assay for Na/K ATPase α1. The Western blot outputs from the capillary Western chromatography are provided in Supplementary Fig. 2. The SS fraction contained more of both GAPDH (106,334 ± 2,742 vs. 20,286 ± 1,113 arbitrary units; $P < 0.001$) and Na/K ATPase α1 (9,535 ± 1,432 vs. 4,049 ± 1,108 arbitrary units; $P < 0.05$) than the IMF fraction.

Muscle Ceramide Concentrations

The concentrations of the ceramide species in the SS and IMF fractions did not differ among the first, second, and third biopsies. We therefore used the average of the three concentrations to represent each individual's muscle ceramide content. These data are provided in Table 2. We found that, with the exception of C14:0-Cer and C18:1-Cer, ceramide concentrations were greater in SS than IMF fractions.

Relationships Among Metabolic Parameters, Body Fat Distribution, and Intramyocellular Subcellular Ceramide Concentrations

Plasma insulin concentrations and HOMA of insulin resistance (HOMA-IR) were positively correlated with SS C16:0 and C18:1 ceramide concentrations (Table 3 and Fig. 2), whereas we did not see similar relationships between these metabolic parameters and SS C14:0-Cer, C20:0-Cer, C24:0-Cer, and C24:1-Cer concentrations. Fasting plasma triglyceride concentrations were positively correlated with SS C18:1-Cer concentrations (γ = 0.389; P = 0.001). There was no significant correlation between plasma palmitate concentrations and SS ceramide concentrations. The IMF ceramide concentrations did not correlate with any metabolic parameters (Table 3).

In general, there were no strong relationships between body composition parameters and intramyocellular ceramide concentrations. Although percent body fat correlated positively and significantly with SS C16:0 ceramide concentration, the P value did not reach our threshold for statistical significance (γ = 0.311; P = 0.011). Visceral fat mass correlated positively with SS C18:1 ceramide concentrations and met our stricter definition for statistical significance (γ = 0.366; P = 0.002). There were no relationships between the IMF ceramide subspecies concentrations and body fat or body fat distribution.

To test whether the ceramide subspecies concentrations in SS compartments are independently associated with metabolic parameters, we performed multivariate linear regression analysis with ceramide subspecies concentrations as the dependent variable and age, sex, HOMA-IR, plasma triglyceride, and visceral fat mass as independent variables. HOMA-IR was an independent predictor (β = 0.429; P = 0.0004) of SS C16:0 ceramide concentrations, and plasma triglyceride concentrations were an independent predictor (β = 0.389; P = 0.0013) of SS C18:1 ceramide concentrations.

Fractional Contribution of De Novo Synthesis to Intramyocellular Ceramides

Plasma [U-^{13}C]palmitate enrichments were stable between the first and second biopsies (Table 4). Between the first and second biopsies (while the [U-^{13}C]palmitate infusion was continuing), the [$^{13}C_{16}$]16:0 ceramide enrichment increased significantly in both SS and IMF (Table 4). The fractional contribution of plasma palmitate to intramyocellular 16:0 ceramide was greater in SS than IMF fractions at the time of both the first and second muscle biopsies (Table 4).

Table 3—Relationships between metabolic parameters and intramyocellular ceramide concentrations

	Insulin*		HOMA-IR*		Triglyceride*	
Ceramide	γ	*P* value	γ	*P* value	γ	*P* value
SS fraction						
Total Cer	0.133	0.286	0.145	0.250	0.177	0.158
C14:0-Cer	−0.085	0.499	−0.009	0.944	0.009	0.942
C16:0-Cer	0.413	0.0006[a]	0.429	0.0004[a]	0.269	0.030
C18:1-Cer	0.323	0.0082[a]	0.359	0.003[a]	0.389	0.001[a]
C18:0-Cer	0.219	0.078	0.255	0.041	0.285	0.021
C20:0-Cer	0.140	0.264	0.108	0.391	0.003	0.983
C24:1-Cer	−0.084	0.504	−0.082	0.517	−0.034	0.785
C24:0-Cer	−0.165	0.186	−0.199	0.112	−0.115	0.363
IMF fraction						
Total Cer*	0.020	0.871	0.030	0.811	0.069	0.586
C14:0-Cer*	−0.063	0.618	−0.043	0.731	−0.066	0.600
C16:0-Cer*	0.102	0.414	0.124	0.324	0.151	0.231
C18:1-Cer*	0.180	0.149	0.210	0.108	0.200	0.110
C18:0-Cer	−0.005	0.969	−0.008	0.947	0.029	0.816
C20:0-Cer*	−0.042	0.740	−0.069	0.584	−0.164	0.191
C24:1-Cer*	−0.049	0.698	−0.047	0.712	0.010	0.936
C24:0-Cer*	−0.085	0.497	−0.081	0.523	−0.035	0.783

Pearson correlation coefficient (γ) is provided. Intramyocellular ceramide concentrations are the average from the three biopsies and normalized to milligrams protein. *Data were log-transformed prior to analysis. [a]Statistically significant relationship after the modified adjustment for multiple species comparisons.

The data from the second biopsy were used to calculate the fractional contribution of plasma palmitate to intramyocellular 16:0 ceramide for subsequent analyses.

We assessed whether the fraction of intramyocellular C16:0 ceramide that was derived from de novo synthesis using plasma palmitate was related to the C16:0 ceramide pool size, plasma palmitate concentrations, and/or the metabolic parameters noted above. If the contribution of de novo C16:0 ceramide synthesis from plasma palmitate was similar for all individuals, we predicted that the fraction of the C16:0 ceramide pool derived from [U-^{13}C]palmitate would be less in those with greater intramyocellular C16:0 ceramide content as a result of the dilution of newly synthesized ceramides into a large pool of pre-existing ceramides. Instead, we found a positive relationship between the fractional contribution of plasma palmitate and the SS C16:0 ceramide (γ = 0.435; *P* = 0.002) (Fig. 3*A*), but not IMF C16:0, concentration (γ = −0.232; *P* = 0.109). We also reasoned that, all things being equal, if FFA concentrations drive de novo muscle ceramide synthesis, there would be a positive correlation between plasma palmitate concentrations and the fraction of the C16:0 ceramide pool observed to come from [U-^{13}C]palmitate. There was no significant relationship between plasma palmitate concentrations and the fraction of intramyocellular C16:0 ceramide that was derived from de novo synthesis from plasma palmitate (γ = 0.112, *P* = 0.410 for SS; γ = 0.023, *P* = 0.864 for IMF).

Plasma insulin concentrations and HOMA-IR were significantly correlated with fractional contribution of plasma palmitate to intramyocellular SS 16:0 ceramide (γ = 0.375, *P* = 0.004; and γ = 0.377, *P* = 0.004, respectively) (Fig. 3*B*), whereas plasma glucose concentrations were correlated with fractional contribution of plasma palmitate to intramyocellular IMF 16:0 ceramide (γ = 0.280; *P* = 0.037). There were no significant relationships between body fat distribution and fractional contributions of plasma palmitate to intramyocellular 16:0 ceramide in either subcellular location.

To determine the predictors that related to fractional contributions of plasma palmitate to intramyocellular 16:0 ceramide, we performed multivariate regression analysis with fractional contribution of plasma palmitate as the dependent variable and age, sex, plasma insulin, plasma glucose, plasma palmitate, and visceral fat mass as independent variables. For fractional contributions of plasma palmitate to intramyocellular SS 16:0 ceramide, plasma insulin concentrations were a significant predictor (β = 0.375; *P* = 0.0044). For fractional contribution of plasma palmitate to intramyocellular IMF 16:0 ceramide, plasma glucose concentrations and sex (male vs. female) were significant predictors (β = 0.392, *P* = 0.0038; and β = −0.363, *P* = 0.0070, respectively).

DISCUSSION

Because intramyocellular ceramides have been causally linked to muscle insulin resistance, we investigated the relationships between the subcellular location of different muscle ceramide species and parameters of body composition and insulin resistance. In addition, we assessed the relationships between these metabolic conditions and the fractional contribution of plasma palmitate to intramyocellular SS and IMF 16:0 ceramide. Our primary findings were: *1*) the associations between intramyocellular ceramide concentrations and hyperinsulinemia/hypertriglyceridemia were largely limited to the SS subcellular fraction; *2*) SS ceramides with 16 and 18 carbon fatty acids, but not other ceramide species

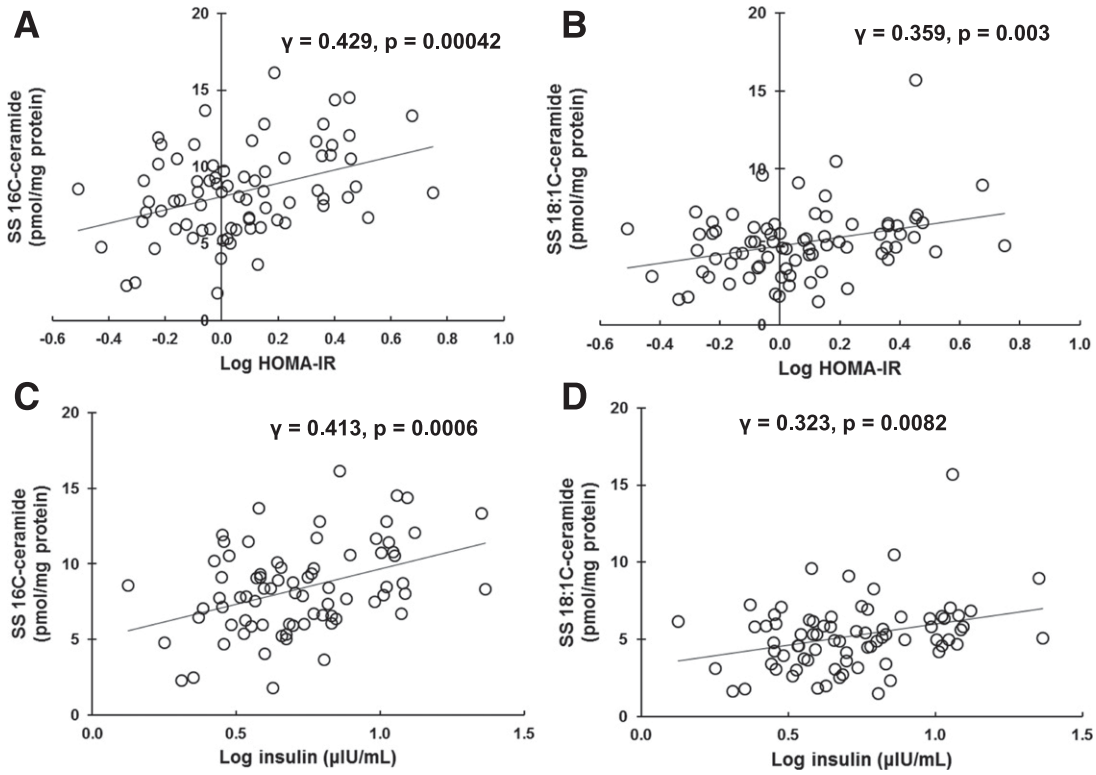

Figure 2—Relationships between clinical parameters and ceramide subspecies in SS compartments. *A*: Correlation between HOMA-IR and SS 16C-ceramide concentration. *B*: Correlation between HOMA-IR and SS 18:1C-ceramide concentration. *C*: Correlation between plasma insulin concentration and SS 16C-ceramide concentration. *D*: Correlation between plasma insulin concentration and SS 18:1C-ceramide concentrations. Intramyocellular ceramide concentrations are the average from the three biopsies and normalized to milligrams protein. Log-transformed values were used for normal distribution.

concentrations, were positively correlated with markers of insulin resistance; *3*) plasma insulin concentrations (and indices of insulin resistance) were independently related to the fractional contribution of plasma palmitate to SS 16:0 ceramides; and *4*) fractional contribution of plasma palmitate to intramyocellular SS 16:0 ceramide was positively correlated with SS ceramide concentrations.

The ceramide content of skeletal muscle has been reported to be increased in obese insulin-resistant individuals and in men at risk for developing type 2 diabetes (3,4). These increased concentrations may be causally related to impaired insulin sensitivity (3,17), as supported by the findings showing inhibition of protein kinase B/Akt by ceramide via atypical protein kinase C or protein phosphatase-2A (18,19). However, despite strong evidence from in vitro and animal studies (2), there have been mixed reports regarding skeletal muscle ceramide content and insulin resistance in humans (3,17,20). One possible explanation is that ceramide accumulation varies by subcellular location and that the locations affect muscle metabolism differently.

Table 4—Intramyocellular [$^{13}C_{16}$]16:0 ceramide enrichment and fractional contributions of plasma palmitate to intramyocellular ceramide during a continuous intravenous infusion of [U-^{13}C]palmitate

Time from baseline	1.5 h	6.5 h	24 h	*P* value
Plasma [U-^{13}C]palmitate enrichment	0.085 (0.065–0.103)	0.081 (0.065–0.104)		0.457
[$^{13}C_{16}$]16:0 ceramide enrichment				
SS fraction	0.008 (0.000–0.014)	0.014 (0.008–0.020)	0.006 (0.000–0.009)	<0.0001
IMF fraction	0.004 (0.000–0.007)	0.008 (0.006–0.012)	0.000 (0.000–0.006)	<0.0001
Fractional contribution of plasma palmitate to ceramide (%)				
SS fraction	7.5 (0.0–16.4)*	18.2 (8.4–24.8)†		<0.0001
IMF fraction	4.3 (0.0–8.4)	8.7 (6.9–16.1)		<0.0001

Data are median (interquartile range). Plasma [U-^{13}C]palmitate enrichment represents the values between baseline and the first biopsy and between the first biopsy and second biopsy, respectively. Analyzed by Friedman test or Wilcoxon signed-rank test. *Significantly different from the values in IMF at the same time point ($P = 0.0086$). †Significantly different from the values in IMF at the same time point ($P = 0.0006$).

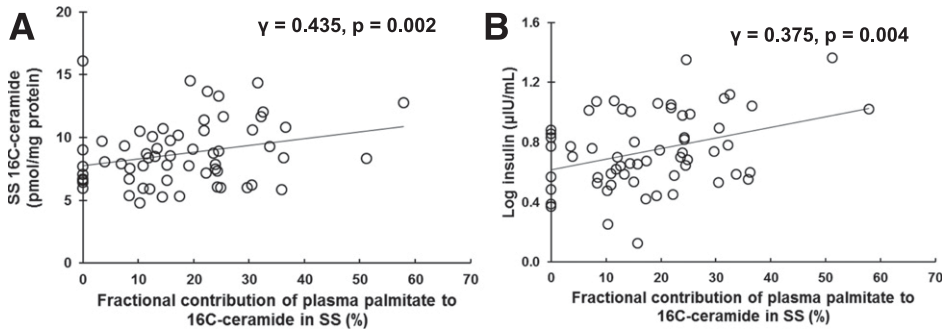

Figure 3—Relationships among intramyocellular ceramide concentrations, plasma insulin concentrations, and fractional contribution of plasma palmitate to intramyocellular ceramides. *A*: Correlation between SS 16C-ceramide concentration and fractional contribution of plasma palmitate to 16C-ceramide in SS fraction. *B*: Correlation between plasma insulin concentration and fractional contribution of plasma palmitate to 16C-ceramide in SS fraction. Intramyocellular ceramide concentrations are the average from the three biopsies and normalized to milligrams protein. Fractional contribution of plasma palmitate was at the time of the second biopsy. Log-transformed values were used for normal distribution.

Most investigators measure the ceramide content in whole muscle. Our findings that SS, but not IMF, ceramide concentrations were related to insulin resistance parameters may offer an explanation as to why whole-muscle ceramides are not consistently linked with insulin resistance. The steps of the insulin signaling pathway involved in cellular glucose uptake occur at or near the plasma membrane (2,7,21), and our analysis of SS and IMF fractions of skeletal muscle indicate that SS is relatively enriched in plasma membrane (and cytosol) compared with the IMF fraction. In addition, the ceramide-rich region within the membrane might be important in mediating insulin signaling (22). Our data suggest that, to the extent that ceramides are linked to defective insulin signaling, the SS compartment is more relevant.

In addition to the subcellular location of ceramide, ceramide species with different acyl chains might have distinct functions. We found that insulin resistance markers were positively related only to SS C16:0 and C18:1 ceramide concentrations. We may have falsely labeled as nonsignificant (Table 3) a few positive associations between SS C16:0 and C18:0 ceramide concentrations and markers of insulin resistance by using a Bonferroni correction factor. The general trend for the C16 and C18 species to be positively associated with these markers argues for their inclusion among the "suspect" ceramide species and suggests our correction factor was overly strict. The strong relationship between SS C16:0 ceramide concentration and insulin resistance markers observed in the current study is consistent with findings from in vitro studies showing C16:0 ceramide binds and activates protein kinase C-ζ, which antagonizes protein kinase B/Akt signaling (23). A previous study of obese women also indicated that skeletal muscle C16:0 ceramide concentrations in human total skeletal muscle cell homogenate were inversely related to insulin action as measured by a hyperinsulinemic-euglycemic clamp (24). Other reports suggest that C16:0 ceramides also inhibit mitochondrial electron transport and inhibit β-oxidation (25). Although it has been reported that C18:0 ceramide is inversely related to insulin sensitivity in humans (26), our results indicated that the relationship between SS C18:0 ceramide concentration and insulin resistance markers was not as strong ($\gamma = 0.255$; $P = 0.041$). The differences in the findings might result, partly, from the differences in study participants. Compared with our study participants, the subjects in that previous study (26) consisted of obese individuals, endurance-trained athletes, and subjects with type 2 diabetes. Interestingly, we found that SS C18:1 ceramide concentrations were independently associated with plasma triglyceride levels in multivariate regression analysis. Increased plasma triglycerides and FFA have long been considered to be related to insulin resistance in humans (27). In the fasting conditions, muscle lipid accumulation could result from fatty acid oversupply, originating either from very LDL (VLDL)-triglyceride or FFA released from adipose tissue (28). In humans, lipoprotein lipase-mediated fatty acid uptake might be sufficient in skeletal muscle to provide fatty acids for ceramide synthesis (29).

We were surprised by the lack of relationship between palmitate concentrations and SS ceramide concentrations, as well as the lack of relationship between palmitate concentrations and the fractional contribution of plasma palmitate to SS C16:0 ceramides. In a previous study using a rodent model of type 1 diabetes, elevated FFA increased the ceramide contents in skeletal muscle subcellular compartments compared with a control condition (30). However, the plasma FFA concentrations >2 mmol/L resulting from insulin deprivation were likely a greater stimulus to de novo ceramide synthesis compared with the control condition than the narrower range of FFA concentrations in our study. Our findings seem to indicate that the difference in whole-body FFA release between lean and moderately obese adults under the overnight fasting conditions is too small to affect muscle ceramide metabolism, a circumstance that could be different in the postprandial state (9). Plasma VLDL-triglyceride also may reflect hepatic insulin resistance related to FFA oversupply to the liver (31,32). We also found that SS C18:1 ceramide concentrations correlated

significantly with visceral fat mass, which is closely linked to adverse metabolic effects (31). However, the relationship between SS C18:1 ceramide concentration and visceral fat mass was no longer significant after adjustment for covariates, suggesting that the amount of visceral fat mass itself is not directly responsible for differences in SS 18:1 ceramide concentrations.

We found that de novo synthesis of skeletal muscle ceramide from plasma FFA could be a significant contributor to ceramides (10), especially in the SS pool. It was interesting to find that the increase in the 16:0 ceramide enrichments from the first to the second biopsies was not proportional to the duration of the tracer infusion. The 16:0 ceramide enrichments in both SS and IMF pools at the time of the second biopsy were approximately twice that found in samples from the first biopsy, whereas the infusion had been continued approximately four times longer. This suggests there may have been a plateau effect taking place. We therefore used the enrichment at the second biopsy as a better indicator of the contribution of plasma palmitate to de novo SS C16:0 ceramides. The lesser enrichment in IMF than SS C 16:0 ceramides may imply that ceramides synthesized for the IMF pool are less dependent on plasma FFA or that ceramides synthesized in the SS compartment slowly equilibrate with the IMF compartment. Our finding of a positive relationship between the SS C16:0 ceramide concentrations and the fractional contribution of plasma palmitate to C16:0 ceramides suggests to us that de novo synthesis of ceramides may be responsible for greater SS ceramide content. However, the lack of association between plasma FFA concentrations and SS ceramides suggests that other factors play a more important role in the postabsorptive state. We also found that the fractional contribution of plasma palmitate to SS C16:0 ceramides was positively correlated with fasting plasma insulin concentrations. From our data, it is not possible to derive cause and effect. One explanation is that hyperinsulinemia can drive de novo ceramide synthesis, but another is that greater amounts of newly synthesized ceramides from plasma FFA are causally related to muscle insulin resistance (Fig. 4). Straczkowski et al. (24) found that 4 h of hyperinsulinemia did not result in an increase in ceramide concentrations in skeletal muscle in humans. Although this may seem to argue against the former explanation, plasma FFA concentrations are typically suppressed during an insulin clamp, which might offset any effects of insulin on de novo ceramide synthesis. Our analysis indicated that plasma glucose concentrations were independently associated with the fractional contribution of plasma palmitate to IMF 16:0 ceramide. We could find no literature that might explain such an association and should caution that this finding could represent a type 1 statistical error despite our attempts to adjust for multiple comparisons.

The intramyocellular [$^{13}C_{16}$]16:0 ceramide enrichment that was achieved in response to the continuous intravenous infusion of [U-^{13}C]palmitate had all but disappeared by the next morning (~18 h after discontinuation of the tracer infusion). This suggests that the pools into which de novo–synthesized ceramides are incorporated turn over at a relatively rapid rate. We do not know if the total ceramide pools turn over with equal rapidity, however.

We can envision several models to explain the associations we observed between intramyocellular ceramides in insulin resistance (Fig. 4). Cytosolic and plasma membrane (SS) ceramides with 16 and 18 carbon fatty acids contribute to defective insulin signaling (2,7,21). The lack of relationships between plasma palmitate concentrations and SS ceramide concentrations, as well as the lack of relationship between plasma palmitate concentrations and the fractional contribution of plasma palmitate to SS C 16:0 ceramides, suggests that the relatively narrow range of FFA concentrations seen after an overnight fast does not drive de novo synthesis and accumulation of SS ceramides. Instead, either hyperinsulinemia stimulates de novo ceramide synthesis or newly synthesized C 16 ceramides uniquely contribute to impaired insulin action.

This study has some limitations. Because we involved participants with a wide range of BMIs, this likely affected the intramyocellular lipids before the dietary control period. This study design allowed us to evaluate the relationship among body fat, metabolic signatures, and intramyocellular ceramides independent of the immediate antecedent diet. It is possible that the 5-day diet control the volunteers received to ensure energy and macronutrient balance could have affected the composition of intramyocellular lipids (33). The diet-control period was designed to eliminate the day-to-day variation in energy intake that can affect FFA metabolism and to provide a consistent macronutrient pattern (50% carbohydrate, 35% fat, and 15% protein) for all participants. However, our volunteers consumed essentially the same types of foods as their typical, individual diets, but in more consistent amounts and balanced with regard to protein, fat, and carbohydrate. This approach seems less likely to fundamentally alter intramyocellular lipids. We note that Helge et al. (34) found that skeletal muscle ceramide content did not differ after 3 weeks of a high- or low-fat diet in patients with type 2 diabetes. We measured insulin resistance index using HOMA-IR, which, although reasonably well correlated with insulin resistance from the hyperinsulinemic-euglycemic clamp (35,36), does not separate the direct impact of skeletal muscle on insulin sensitivity. However, offsetting the somewhat imperfect measures of insulin resistance, we had a relatively large study population and performed three biopsies over 24 h. This likely allowed us to detect associations that would have been missed had we studied fewer volunteers or done a single biopsy. We acknowledge that we might have missed some associations because we did not have more robust insulin-resistance measures. In addition, our conclusion that C16 and C18 ceramide species concentrations were associated with markers of insulin resistance, whereas C20–C24 ceramides were not, could be because of the overestimates of C20–C24 concentrations we found as a result of not including a species-specific internal standard. However, provided the overestimate is consistent,

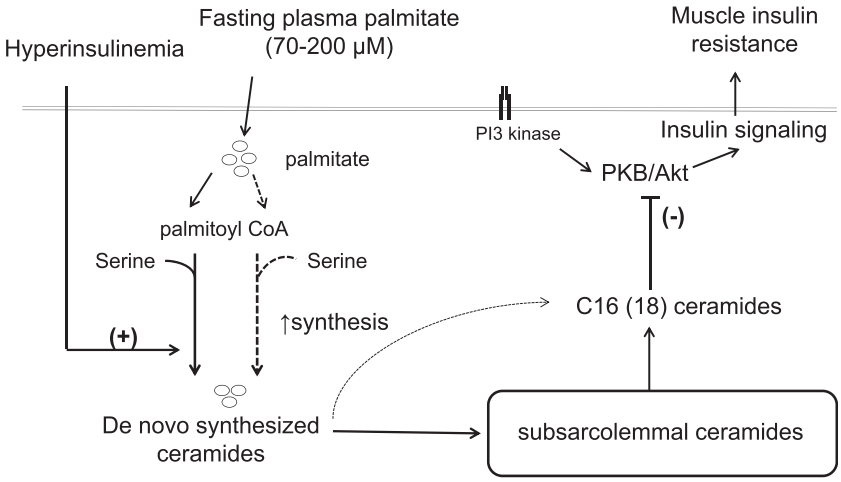

Figure 4—Schema depicting roles of SS ceramides in insulin resistance under postabsorptive conditions. There are two possible explanations for the data regarding SS ceramide concentrations and de novo synthesis of ceramides to insulin resistance. One model depicts the circumstance in which, when plasma palmitate concentrations are between 70 and 200 μmol/L, de novo ceramide synthesis is largely driven by intracellular processes that are stimulated by insulin, not by plasma palmitate availability. This possibility is depicted by the solid arrows showing the path of ceramide synthesis and action. In this scenario, insulin drives the accumulation of SS 16C-18C ceramides that can further interfere with insulin signaling. The other model (dashed arrows) depicts the circumstance in which intramyocellular processes, not plasma palmitate concentrations, are the primary driver of de novo ceramide synthesis in SS fraction. These newly synthesized 16C-18C ceramides are uniquely able to impair insulin signaling and also contribute to SS ceramide accumulation. PKB, protein kinase B; PI3, phosphoinositide 3.

the presence or absence of a correlation should still be meaningful. Unfortunately, we do not have sufficient remaining samples from this study to reanalyze the ceramide concentrations using the more specific internal standard. In the current study, the enrichment in the IMF was often at or below the limit of accurate measurement using our approach. The lack of significant findings regarding IMF de novo ceramide synthesis could be because of the greater assay noise at very low enrichments. However, knowing that the contribution of de novo–synthesized ceramides in IMF is substantially less than SS remains a helpful observation for planning future studies. Finally, we note that plasma palmitate that is taken up by the liver might be released into the circulation as labeled VLDL-triglyceride fatty acids and enter skeletal muscle. The relative contributions of VLDL–^{13}C-palmitate to C16:0 ceramide at the later time points cannot be discerned.

In summary, this is the first report to show that the subcellular location of ceramide and types of ceramide species in skeletal muscle are related to insulin resistance in humans. In addition, the metabolic milieu might further reflect the de novo synthesis of intramyocellular ceramide from plasma palmitate in the fasting condition.

Acknowledgments. The authors thank the research volunteers for participating and the following Mayo Clinic (Rochester, MN) employees: Barb Norby, Carley Vrieze, Christy Allred, Debra Harteneck, Darlene Lucas, Lendia Zhou, and the Mayo Clinic CRU nursing staff.

Funding. This work was supported by U.S. Public Health Service grants from the National Institute of Diabetes and Digestive and Kidney Diseases (DK-40484, DK-45343, DK-50456, and R-00585) and by the Mayo Foundation.

Duality of Interest. No potential conflicts of interest relevant to this article were reported.

Author Contributions. J.O.C. and K.C.H. researched data and wrote the manuscript. C.K. performed the studies, researched data, and reviewed and edited the manuscript. A.U.B.-Z. planned and performed sample analysis and reviewed and edited the manuscript. M.D.J. designed the study and reviewed and edited the manuscript. M.D.J. is the guarantor of this work and, as such, had full access to all the data in the study and takes responsibility for the integrity of the data and the accuracy of the data analysis.

References

1. Summers SA. Ceramides in insulin resistance and lipotoxicity. Prog Lipid Res 2006;45:42–72

2. Chavez JA, Summers SA. A ceramide-centric view of insulin resistance. Cell Metab 2012;15:585–594

3. Adams JM 2nd, Pratipanawatr T, Berria R, et al. Ceramide content is increased in skeletal muscle from obese insulin-resistant humans. Diabetes 2004;53:25–31

4. Straczkowski M, Kowalska I, Baranowski M, et al. Increased skeletal muscle ceramide level in men at risk of developing type 2 diabetes. Diabetologia 2007;50:2366–2373

5. Bergman BC, Hunerdosse DM, Kerege A, Playdon MC, Perreault L. Localisation and composition of skeletal muscle diacylglycerol predicts insulin resistance in humans. Diabetologia 2012;55:1140–1150

6. Nielsen J, Mogensen M, Vind BF, et al. Increased subsarcolemmal lipids in type 2 diabetes: effect of training on localization of lipids, mitochondria, and glycogen in sedentary human skeletal muscle. Am J Physiol Endocrinol Metab 2010;298:E706–E713

7. Larsen PJ, Tennagels N. On ceramides, other sphingolipids and impaired glucose homeostasis. Mol Metab 2014;3:252–260

8. Grösch S, Schiffmann S, Geisslinger G. Chain length-specific properties of ceramides. Prog Lipid Res 2012;51:50–62

9. Jensen MD. Role of body fat distribution and the metabolic complications of obesity. J Clin Endocrinol Metab 2008;93(Suppl. 1):S57–S63

10. Blachnio-Zabielska AU, Persson X-MT, Koutsari C, Zabielski P, Jensen MD. A liquid chromatography/tandem mass spectrometry method for measuring the in vivo incorporation of plasma free fatty acids into intramyocellular ceramides in humans. Rapid Commun Mass Spectrom 2012;26:1134–1140

11. Jensen MD, Kanaley JA, Reed JE, Sheedy PF. Measurement of abdominal and visceral fat with computed tomography and dual-energy x-ray absorptiometry. Am J Clin Nutr 1995;61:274–278
12. Persson X-MT, Blachnio-Zabielska AU, Jensen MD. Rapid measurement of plasma free fatty acid concentration and isotopic enrichment using LC/MS. J Lipid Res 2010;51:2761–2765
13. Humphreys SM, Fisher RM, Frayn KN. Micro-method for measurement of sub-nanomole amounts of triacylglycerol. Ann Clin Biochem 1990;27:597–598
14. Guo Z, Mishra P, Macura S. Sampling the intramyocellular triglycerides from skeletal muscle. J Lipid Res 2001;42:1041–1048
15. Jaleel A, Short KR, Asmann YW, et al. In vivo measurement of synthesis rate of individual skeletal muscle mitochondrial proteins. Am J Physiol Endocrinol Metab 2008;295:E1255–E1268
16. Short KR, Nygren J, Barazzoni R, Levine J, Nair KST. T(3) increases mitochondrial ATP production in oxidative muscle despite increased expression of UCP2 and -3. Am J Physiol Endocrinol Metab 2001;280:E761–E769
17. Coen PM, Dubé JJ, Amati F, et al. Insulin resistance is associated with higher intramyocellular triglycerides in type I but not type II myocytes concomitant with higher ceramide content. Diabetes 2010;59:80–88
18. Powell DJ, Hajduch E, Kular G, Hundal HS. Ceramide disables 3-phosphoinositide binding to the pleckstrin homology domain of protein kinase B (PKB)/Akt by a PKCzeta-dependent mechanism. Mol Cell Biol 2003;23:7794–7808
19. Mahfouz R, Khoury R, Blachnio-Zabielska A, et al. Characterising the inhibitory actions of ceramide upon insulin signaling in different skeletal muscle cell models: a mechanistic insight. PLoS One 2014;9:e101865
20. Skovbro M, Baranowski M, Skov-Jensen C, et al. Human skeletal muscle ceramide content is not a major factor in muscle insulin sensitivity. Diabetologia 2008;51:1253–1260
21. Andjelković M, Alessi DR, Meier R, et al. Role of translocation in the activation and function of protein kinase B. J Biol Chem 1997;272:31515–31524
22. Stancevic B, Kolesnick R. Ceramide-rich platforms in transmembrane signaling. FEBS Lett 2010;584:1728–1740
23. Müller G, Ayoub M, Storz P, Rennecke J, Fabbro D, Pfizenmaier K. PKC zeta is a molecular switch in signal transduction of TNF-alpha, bifunctionally regulated by ceramide and arachidonic acid. EMBO J 1995;14:1961–1969
24. Straczkowski M, Kowalska I, Nikolajuk A, et al. Relationship between insulin sensitivity and sphingomyelin signaling pathway in human skeletal muscle. Diabetes 2004;53:1215–1221
25. Hla T, Kolesnick R. C16:0-ceramide signals insulin resistance. Cell Metab 2014;20:703–705
26. Bergman BC, Brozinick JT, Strauss A, et al. Muscle sphingolipids during rest and exercise: a C18:0 signature for insulin resistance in humans. Diabetologia 2016;59:785–798
27. Schalch DS, Kipnis DM. Abnormalities in carbohydrate tolerance associated with elevated plasma nonesterified fatty acids. J Clin Invest 1965;44:2010–2020
28. Eckel RH. Lipoprotein lipase. A multifunctional enzyme relevant to common metabolic diseases. N Engl J Med 1989;320:1060–1068
29. Miles JM, Park YS, Walewicz D, et al. Systemic and forearm triglyceride metabolism: fate of lipoprotein lipase-generated glycerol and free fatty acids. Diabetes 2004;53:521–527
30. Zabielski P, Blachnio-Zabielska A, Lanza IR, et al. Impact of insulin deprivation and treatment on sphingolipid distribution in different muscle subcellular compartments of streptozotocin-diabetic C57Bl/6 mice. Am J Physiol Endocrinol Metab 2014;306:E529–E542
31. Ebbert JO, Jensen MD. Fat depots, free fatty acids, and dyslipidemia. Nutrients 2013;5:498–508
32. Fabbrini E, Sullivan S, Klein S. Obesity and nonalcoholic fatty liver disease: biochemical, metabolic, and clinical implications. Hepatology 2010;51:679–689
33. Kien CL, Everingham KI, D Stevens R, Fukagawa NK, Muoio DM. Short-term effects of dietary fatty acids on muscle lipid composition and serum acylcarnitine profile in human subjects. Obesity (Silver Spring) 2011;19:305–311
34. Helge JW, Tobin L, Drachmann T, Hellgren LI, Dela F, Galbo H. Muscle ceramide content is similar after 3 weeks' consumption of fat or carbohydrate diet in a crossover design in patients with type 2 diabetes. Eur J Appl Physiol 2012;112:911–918
35. Matthews DR, Hosker JP, Rudenski AS, Naylor BA, Treacher DF, Turner RC. Homeostasis model assessment: insulin resistance and beta-cell function from fasting plasma glucose and insulin concentrations in man. Diabetologia 1985;28:412–419
36. Bonora E, Targher G, Alberiche M, et al. Homeostasis model assessment closely mirrors the glucose clamp technique in the assessment of insulin sensitivity: studies in subjects with various degrees of glucose tolerance and insulin sensitivity. Diabetes Care 2000;23:57–63